ORIGINAL PAPER

Cristian Linares · Daniela Geraldo · Maritza Paez · José H. Zagal

Non-linear correlations between formal potential and Hammett parameters of substituted iron phthalocyanines and catalytic activity for the electro-oxidation of hydrazine

Abstract The activity of the different iron phthalocyanines was examined using the complexes adsorbed on graphite electrodes. The effect of the Fe(II)/(I) formal potential of iron phthalocyanines on the their catalytic activity for the electro-oxidation of hydrazine was investigated. A plot of log k (rate constant at constant potential) versus the Fe(II)/(I) formal potential gives a volcano curve. The rate of the reaction increases with the driving force of the catalyst (measured as its formal potential) and then decreases for higher driving forces. A similar graph is obtained with a plot of log k versus the sum of the Hammett parameters of the substituents on the periphery of the phthalocyanine ligand. A maximum activity is obtained for a complexes having an M(II)/(I) redox potential close to −0.6 V which agrees with previous studies conducted with phthalocyanines of different metals and with cobalt phthalocyanines bearing different substituents.

Keywords Hydrazine oxidation · Iron phthalocyanines · Electrocatalysis · Volcano plots · Hammett parameters

Introduction

Hydrazine and derivatives have applications as corrosion inhibitors, antioxidants, reducing agents, emulsifiers, herbicides, plant-growth regulators, explosives,

rocket propellants and in fuel cells [1, 2]. The overpotential of the electro-oxidation of hydrazine strongly depends on the electrode material and generally noble metals exhibit high activity for this reaction [3], so it is of crucial importance to find less expensive catalysts for this reaction.

On the other hand, metallophthalocyanines are versatile compounds that exhibit catalytic activity for a great variety of electrodic reactions including the electro-oxidation of hydrazine [4, 5]. Confined on electrodic surfaces they act as mediators for many electron transfer reactions, providing sites for the reacting molecules to interact, lowering the activation energy. This is reflected in the lowering of the overpotential for a given reaction compared to the unmodified electrode. Several authors [4, 6, 7, 8, 9, 10, 11] have correlated the activity of these complexes with their redox potential since this will contribute to the free energy of the reaction and probably to the free energy of activation. In fact "tuning" the redox potential of these complexes by changing the metal or changing the substituents on the ligand has been suggested as a strategy for optimizing their activity for a particular reaction [5].

Linear correlations have been found between the M(II)/(I) formal potential of the metallophthalocyanine and the catalytic activity (measured as rate constant or current at constant applied potential) for the oxidation of 2-mercaptoethanol [12, 13, 14], for the reduction of dihydroxydimercaptodisulfide [15] and for the reduction of O_2 [4, 6, 7, 11, 16, 17] for families of substituted and unsubstituted phthalocyanines of cobalt and of iron. One interesting feature in these correlations is that, with the exception of the reduction of dihydroxydimercaptodisulfide [15], when plotting log I or log k (I are currents and k rate constants taken at constant potential) versus the formal potential of the catalyst, the activity decreases with the driving force of the phthalocyanine, i.e. for oxidation reactions the activity decreases with the oxidizing power of the catalyst [12, 13, 14] and the reverse is observed for reduction reactions [11, 13, 16, 17]. However, in a recent study [18] of the oxidation of

C. Linares · D. Geraldo · M. Paez · J. H. Zagal (✉)
Facultad de Química y Biología,
Universidad de Santiago de Chile, Casilla 40,
Correo 33, Santiago, Chile
E-mail: jzagal@lauca.usach.cl
Tel.: +56-2-6820632
Fax: +56-2-681-2108

2-mercaptoethanol that included cobalt porphyrins and cobalt phthalocyanines with Co(II)/(I) redox potentials ranging from −1.2 to −0.6 V versus SCE in contrast to our previous findings for this reaction [12, 13, 14] we obtained a volcano correlation between log k and the formal potential of the catalysts. So it is possible that the linear correlations found for several reactions [6, 7, 11, 12, 13, 14, 15, 16, 17, 19, 20] could be part of an incomplete volcano if the redox potentials of the catalysts studied do not cover a wide range of values. In a recent study, when investigating the effect of the formal redox potential on the catalytic activity for the electro-oxidation of hydrazine of cobalt phthalocyanines bearing both electron donor and electron acceptor groups on the periphery of the ligand, we found volcano-shaped correlations, where a maximum activity is obtained for Co-phthalocyanine (with no substituents on the ligand) which has a formal redox potential of the Co(II)/I(I) centered around −0.65 V versus SCE [21]. This prompted us to explore these correlations using another metal in the phthalocyanine. In this work we study the electro-oxidation of hydrazine mediated by Fe-phthalocyanine and several derivatives substituted with both acceptor and donor groups on the ligand, in order to have a wide range of formal potentials and to modulate the electron density on the Fe center.

Experimental

Iron phthalocyanine (Fe-Pc), and iron hexadecachlorophthalocyanine (FeCl$_{16}$Pc) were obtained from Aldrich and purified by vacuum sublimation. Iron octamethoxyphthalocyanine (FeOMe-OPc) and iron tetracarboxyphthalocyanine (FeTCPc) were obtained from Professor A.A. Tanaka (Universidade Federal do Maranhao, Brazil). Iron tetraaminophthalocyanine (FeTAPc), and iron tetranitrophthalocyanine (FeTNPc) were obtained from Mid Century Chemicals (U.S.A.) and used as provided. Iron tetrasulfophthalocyanine (FeTSPc) was synthesized and purified according to a method described in the literature [22].

A BAS CV-50w voltammetric analyzer was used for the electrochemical measurements. The working electrode was an ordinary pyrolytic graphite disk (OPG) of 0.44 cm^2 from Pine Instruments and was polished with 800 and 1,200 grit emery paper and 1-μm alumina followed by ultrasonic treatment in purified water for 2 min before use. The reference electrode was a saturated calomel (SCE) electrode and the auxiliary electrode was a platinum (99.99%, Aldrich) spiral wire of 10 cm^2. The electrolyte was 0.2 M NaOH prepared from deionized, double-distilled water, and de-aerated with ultra pure N$_2$. NaOH was analytical grade from Merck. Hydrazinium sulfate from Merck was used for preparing the hydrazine solutions. The graphite surface was modified by placing a drop of 10^{-4} M solution of the complex on the electrode for 30 min. The solvent was dimethyl formamide for FeCl$_{16}$Pc, FeTNPc and FePc, pyridine for FeOMeOPc, FeTAPc and water for FeTSPc and FeTCPc. Adsorption of all complexes was verified by the appearance of typical current peaks in the cyclic voltammograms of the modified electrodes [5, 12, 13, 14, 23].

Results and discussion

The structure of the different iron phthalocyanines investigated is shown in Fig. 1 and depicts the location
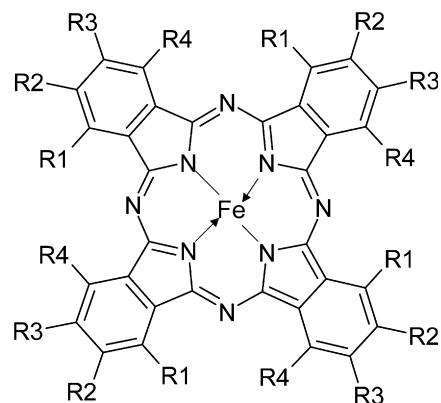
FeOMeOPc: R$_1$=R$_4$= -H, R$_2$=R$_3$= -OCH$_3$
FeTAPc : R$_1$= R$_4$= -H, R$_2$ or R$_3$ = -NH$_2$
FeTCPc : R$_1$ = R$_4$ = -H, R$_2$ or R$_3$ = -CO$_3$
FePc : R$_1$= R$_2$= R$_3$ = R$_4$= -H
FeTSPc : R$_1$= R$_4$ =H, R$_2$ or R$_3$ = -SO$_3$
FeTNPc : R$_1$= R$_4$=H, R$_2$ or R$_3$= -NO$_2$
FeCl16Pc : R$_1$= R$_2$= R$_3$ = R$_4$= -Cl

Fig. 1 Structure of iron phthalocyanines used in this work

of the different substituents on the periphery of the ligand. It is important to note here that tetra-substituted phthalocyanines can have one group in position 2 or 3 of each of the benzene rings and are almost invariably mixtures of isomers, randomly distributed. There is no evidence that the individual isomers have significantly different redox potentials [24, 25, 26]. So one can assume that the effect of the substituents is correlated with its *para* substitution parameters, irrespective of its position 2 or 3 in the benzene ring.

Figure 2 illustrates the potentiodynamic response of OPG modified with pre-adsorbed layers of different iron phthalocyanines. All complexes exhibit at least two reversible current peaks between −1.0 and 0.0 V that are assigned to the Fe(II)/(I) and Fe(III)/(II) reversible couples [4, 5, 10, 14]. These peaks are shifted to more negative potentials by electron-donating groups (methoxy in FeOMeOPc, amino in FeTAPc and carboxy groups in FeTCPc) and to more positive potentials by electron-withdrawing substituents (sulfo in FeTSPc, nitro in FeTNPc and chloro in FeCl$_{16}$Pc) compared to FePc as illustrated in Fig. 2.

Hammett parameters can be applied to the analysis of the effect of substituents on the redox potentials of metallophthalocyanines both in the adsorbed state or in solution [5, 13, 14, 15, 16, 24, 25, 26, 27, 28]. Figure 3 is a plot of the potential of peak 1 versus the sum of the Hammett parameters σ of the groups reported in the literature [29]. A linear correlation is obtained, in agreement with previous work with iron phthalocyanines [5, 14] and phthalocyanines of other metals [5, 13, 15, 16, 24, 25, 26, 27, 28]. In the case of the hexadeca substituted FePcCl$_{16}$, the σ parameters correspond to the sum of the Hammett parameters in the *meta* and *para* positions (R$_1$ and R$_4$ are *meta* and R$_2$ and R$_3$ are *para* in Fig. 1) so for this particular complex eight
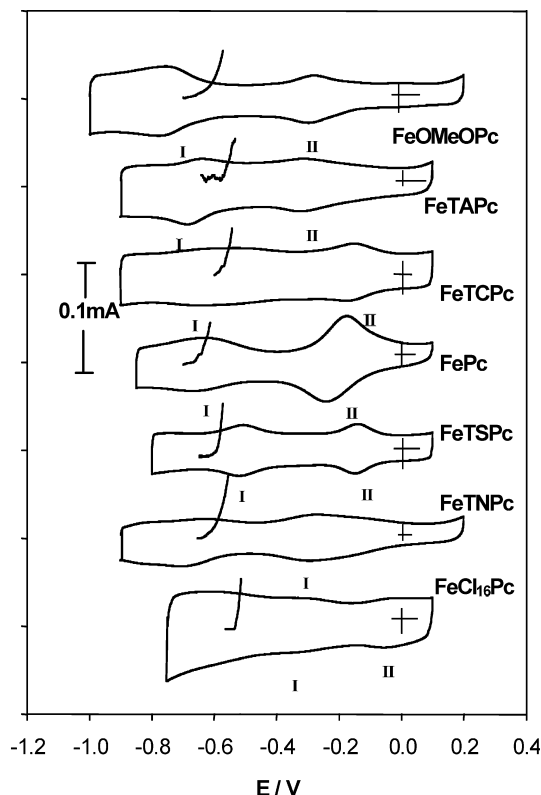
Fig. 2 Cyclic voltammograms of the OPG modified with iron phthalocyanines with different substituents on the periphery of the macrocyclic ring. Effect of substituents. Dashed lines illustrate the foot of the wave for N_2H_4 oxidation after adding 5×10^{-2} M of hydrazine to the electrolyte. Electrolyte pH = 13.0, scan rate 0.3 V s^{-1} for the cyclic voltammograms and 0.005 V s^{-1} for the foot of the wave, N_2 saturated solutions for all curves
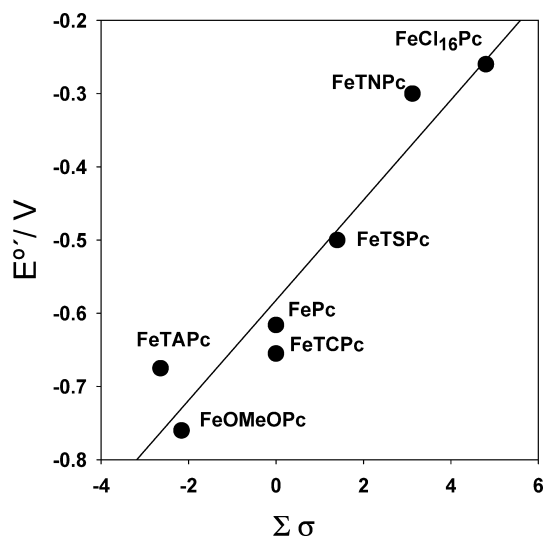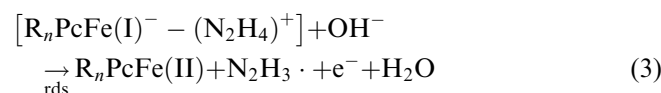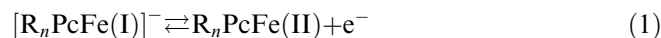

Fig. 3 Plot of the potential of peak 1 in Fig. 2 of the adsorbed iron phthalocyanines derivatives versus the sum of Hammett parameters ($\Sigma\sigma$) of the substituents

chloro groups are located on *meta* and eight chloro groups are located on *para* positions). For all the other complexes the groups are only located on the *para*

position. The surface coverage Γ of the different complexes can be estimated by integrating the charge under peak 1, assuming one electron is transferred per phthalocyanine molecule. However, more accurately, Γ can be determined from the slope of plots of I_p (peak current density) versus v (potential scan rate), since for surface confined species $I_p = n^2F^2v/4RT$. The values obtained for Γ were, in mol cm^{-2}: 4.87×10^{-10} for FeTAPc, 1.16×10^{-10} for FeOMeOPc, 2.47×10^{-10} for FeTCPc, 9.78×10^{-10} for FePc, 5.17×10^{-10} for FeTSPc, 8.24×10^{-10} for FeTNPc, 4.72×10^{-10} for FeCl$_{16}$Pc. In contrast to what was observed with several Co-Pcs [21] there seem to be no correlation between the size of the molecule and the surface coverage, which suggests that not all complexes adsorbed flat on the surface or the way they adsorb on OPG is not the same for all of them.

Figure 2 also shows the foot of the wave corresponding to the oxidation of hydrazine, after adding 5×10^{-2} M N_2H_4 to the electrolyte. When comparing the position of the current peak assigned to the Fe(II)/(I) redox process with the foot of the wave for hydrazine oxidation for each individual phthalocyanine, it can be seen that a simple, direct correlation of these two properties is not obvious as previously observed for the oxidation hydrazine on Co-Pcs [21].

Figure 4 illustrates polarization curves for hydrazine oxidation in the form of Tafel plots, for the different Fe-Pc derivatives. It can be seen here that the activity strongly depends on the nature of the Fe complex. At low polarization the Tafel slopes are close to 0.040 V/decade and gradually change to values close 0.120 V/decade with the exception of FeTSPc that gives a slope of 0.140 V at high polarizations. The bending of the curves at the highest polarizations can be attributed to the formation of N_2 bubbles that block the electrode surface. The slope close to 0.040 V at low polarizations is observed at potentials close to the Fe(II)/(I) couple in the phthalocyanine and suggests that the transfer of a second electron, preceded by a fast electron transfer, is rate controlling. The data can be explained according to the following mechanism:

$$[R_nPcFe(I)]^- \rightleftharpoons R_nPcFe(II) + e^- \tag{1}$$

$$N_2H_4 + R_nPcFe(II) \rightleftharpoons [R_nPcFe(I)^- - (N_2H_4)^+] \tag{2}$$

$$[R_nPcFe(I)^- - (N_2H_4)^+] + OH^-$$
$$\underset{rds}{\rightarrow} R_nPcFe(II) + N_2H_3\cdot + e^- + H_2O \tag{3}$$

$$N_2H_3\cdot \rightarrow N_2H_2\cdot + e^- + H^+ \tag{4}$$

$$N_2H_2\cdot \rightarrow N_2H\cdot + e^- + H^+ \tag{5}$$

$$N_2H\cdot \rightarrow N_2 + e^- + H^+ \tag{6}$$

R_nPcFe represents the different iron phthalocyanines with n substituents R on the periphery of the ligand. The $N_2H_3\cdot$ radical reacts in subsequent steps losing one electron and one proton at the time through steps 4–6 to
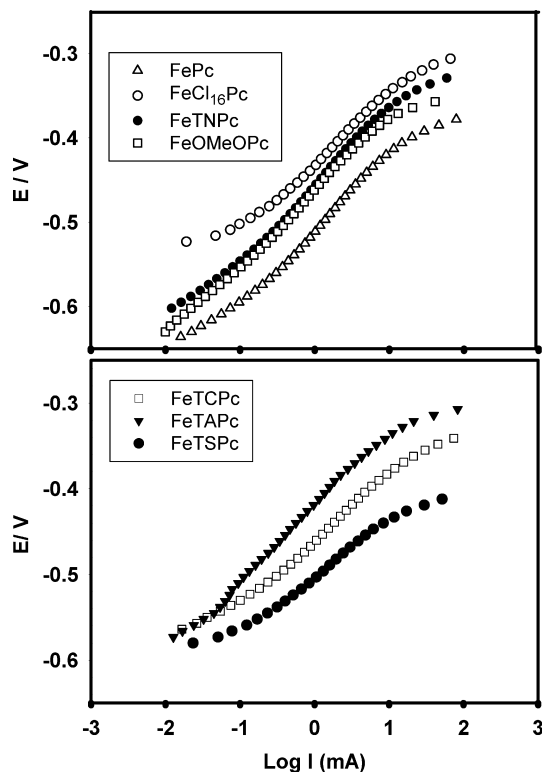
Fig. 4 Tafel plots for the oxidation of hydrazine on OPG modified with different iron phthalocyanines. Data obtained from polarization curves at 5 mV s^{-1} in 0.05 M hydrazine solution in 0.2 M NaOH saturated with N$_2$
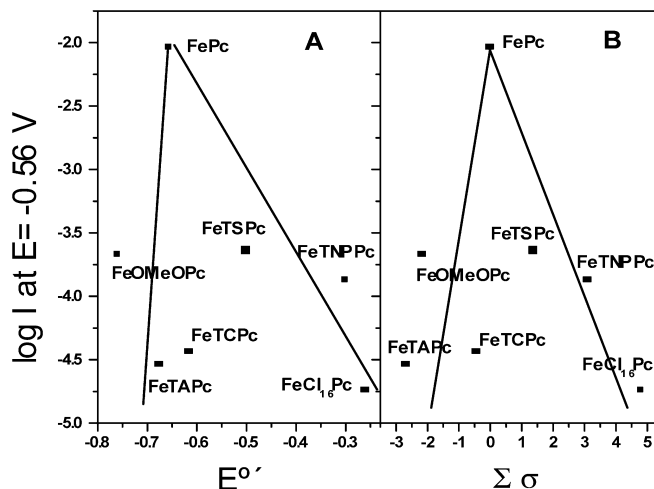

Fig. 5A–B Variation of log I with **A** the formal potential of the catalyst and **B** $\Sigma\sigma$ of the substituents, for the electro-oxidation of hydrazine on iron phthalocyanines with different substituents (data taken from Figs. 3 and 4). I in amps

give nitrogen as the final product of the reaction. Steps occurring after the rate-determining step are not relevant to the Tafel slopes observed. A low Tafel slope should be observed (0.040 V/decade for a symmetry factor equal to 0.5) since the rate determining step (3) is preceded by the fast one-electron transfer step (1), i.e. an ECE mechanism. At potentials where the hydrazine oxidation currents are close to the formal potential of the corresponding R$_n$PcFe(II)/R$_n$PcFe(I) couple (see Fig. 2). the electrode surface is partially covered by R$_n$PcFe(II) species at a concentration, for a given potential, that can be written according to the Nernst equation (applied to surface confined species). If [R$_n$PcFe]$_{ad}$ is the total initial surface concentration of the complex, then:

$$[R_n \, Pc \, Fe(II)]_{ad} = [R_n \, PcFe]_{ad}\theta \qquad 0 < \theta < 1 \qquad (a)$$

$$[R_n \, Pc \, Fe(I)]_{ad} = [R_n \, PcFe]_{ad}(1 - \theta) \qquad (b)$$

Applying the Nernst equation and assuming ideal behavior of the adsorbed species we have:

$$E = E^{o'} + RT/F \ln[\theta/(1 - \theta)] \qquad (c)$$

$$\theta = \frac{\exp\left(E - E^{o'}\right)F/RT}{1 + \exp\left(E - E^{o'}\right)F/RT} \qquad (d)$$

where E is the applied potential and $E^{o'}$ is the formal potential of the [R$_n$PcFe(II)]/[R$_n$PcFe(I)] couple. So, it

can be easily demonstrated that as $(E-E^{o'}) \gg RT/F$, $\theta \rightarrow 1$, i.e. [R$_n$PcFe(II)]$_{ad} \rightarrow$ [R$_n$PcFe]$_{ad}$ and [R$_n$PcFe (I)]$_{ad} \rightarrow 0$. The rate of the reaction expressed as a current would be:

$$I_k = nFAk_3\left[R_n \, Pc \, Fe(I)^- - (N_2H_4)^+\right]_{ad}\exp\alpha\eta F/RT \qquad (e)$$

where k_3 is the rate constant of step 3, η is the overpotential of step 3, n the total number of electrons transferred and A the area of the electrode. All other terms have the usual meaning. The adduct surface concentration is then:

$$\begin{aligned}[R_n \, Pc(-2)M(I)^- &- (N_2H_4)^+]_{ad} \\ &= K_2[R_n \, Pc \, Fe(II)]_{ad}C_{N_2H_4}\end{aligned} \qquad (f)$$

where K_2 is the equilibrium constant for step 2 and $C_{N_2H_4}$ is the concentration of N$_2$H$_4$. Finally, the rate expression can be written as:

$$I_k = nF \, Ak_3K_2[R_n \, Pc \, Fe(II)]_{ad}C_{N_2H_4} \, \exp\left(\alpha\eta F/RT\right) \qquad (g)$$

Since at more positive potentials, [R$_n$PcFe(II)]$_{ad} \rightarrow$ [R$_n$PcFe]$_{ad}$ this term becomes constant and independent of potential. Then, for $\alpha \approx 0.5$, the Tafel slope is $\approx 2RT/F$ or 0.12 V/decade at higher potentials, as observed experimentally.

Figure 5A shows a plot of log I at constant potential versus the Fe(II)/(I) formal potential of the corresponding substituted iron phthalocyanine. Figure 5B shows a plot of log I versus the sum of the Hammett parameters of the substituents located on the periphery of the phthalocyanine ligand. The scattering of the data along the log I axis in the log I versus $E^{o'}$ plot can be attributed to the fact that the different complexes do not all adsorb on the same manner on the graphite or could present different surface orientations. This might not affect very strongly the formal potentials but could affect the electron-transfer reaction rates. Also, there could be
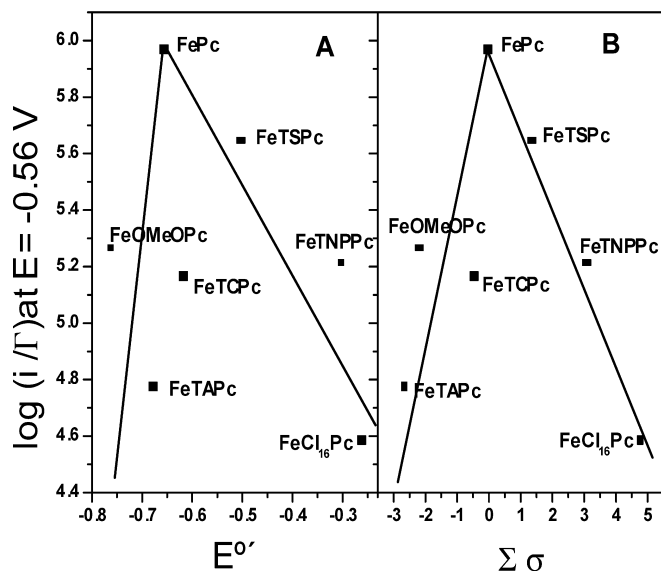
Fig. 6 Variation of log ($i/\Gamma_{complex}$) (currents normalized for the surface concentration of the catalyst) with **A** the formal potential of the catalyst and **B** $\Sigma\sigma$ of the substituents, for the electro-oxidation of hydrazine on iron phthalocyanines with different substituents (data taken from Figs. 3 and 4). i in A cm^{-2} and Γ in mol cm^{-2}

some effect from electronic interactions of the metal center with the π system of the substituted ligand that could affect the catalytic activities which is not necessarily reflected in the redox potential. It can also be argued that, when comparing activities of different iron phthalocyanines, differences in catalyst surface coverage can affect the observed activities. To check this, we have plotted in Fig. 6 essentially the same data of Fig. 5 but normalizing the currents by the surface coverage of each particular catalyst. When comparing the data in Figs. 5 and 6, the data appears less scattered when catalyst surface coverage is taken into account. Two linear correlations are found or better, volcano plots are obtained. For the iron phthalocyanines with the most electron-donating groups, the catalytic activity increases very sharply with the driving force of the catalyst up to a point. As the substituents become more electron-withdrawing, or the formal potential becomes more positive, the catalytic activity decreases. So the data in Figs. 5 and 6 suggest that there is an optimum formal potential or an optimum effect of the substituents on the catalytic activity but also show that, due to the dispersion of the data, there are other factors apart from the redox potential that affect the reactivity of the Fe center. This illustrates the delicate balance involved to obtain a maximum activity. It seems that the optimum formal potential is around −0.65 V versus SCE. This value is close to that found in previous work, when comparing activities of phthalocyanines of different metals (Cr, Mn, Fe and Co) [4, 30] and of several substituted cobalt phthalocyanines [21].

According to the mechanism proposed above, the rate of the reaction will be given by $v = K_2k_3[R_nPcFe(II)]$ [N_2H_4][OH^-]. K_1 is the equilibrium constant of step 1

and k_3 is the rate constant of step 3. The chemical order of the reaction is one in hydrazine and in OH^- ions as found in previous publications [30, 31, 32].

The maximum catalytic activity observed in Figs. 5 and 6 could also be the result of a combined effect of steps 2 and 3 in the mechanism proposed above, which will affect the values of K_2 and k_3. Electron-withdrawing groups will increase K_2 since they will stabilize the Fe(I) state. Electron-donating groups will favor step 3 (they stabilize the Fe(II) state) and increase the value of k_3, which is the rate-determining step. The observed rate constant k is K_2k_3 and shows then a combined effect of both factors. The concave downward volcano correlation of rates versus the sum of the Hammett parameters has been long known to be associated where changing substituent changes the rate-determining step [33]. Even though this explanation seems to be valid for our previous work with cobalt phthalocyanines, it is not applicable to iron phthalocyanines.

We can conclude that, in contrast to what is found for other electrochemical reactions catalyzed by metall-ophthalocyanines, the correlations between the catalytic activity and the formal potential, for phthalocyanines of the same metal with substituents on the periphery of the ring, are not linear but rather follow a volcano type of correlation which agrees with previous work involving cobalt phthalocyanines [21]. The scattering of the data along the log I axis in the log I versus $E^{o'}$ plot might reflect the fact that the different complexes can adopt different surface orientations, depending on the substituents and affecting the reaction rates for each particular phthalocyanine. Also, there could be some effects from electronic interactions of the metal center with the π system of the substituted ligand (metal to ring back bonding) [34] that could affect the rate of electron transfer and the formation of the precursor adduct (step 2). Formation of an adduct between hydrazine and the phthalocyanine has been documented in the literature for cobalt tetrasulfonated phthalocyanine at low temperatures on the basis of electronic spectra and EPR studies which shows that the formation of Co(I) species is involved [35]. It is likely that a similar situation occurs with iron phthalocyanines. We have observed in this work that the open circuit potential of the OPG/R$_n$PcFe electrode shifts to potentials more negative than the Fe(II)/(I) formal potential upon the addition of hydrazine to the electrolyte suggesting the formation of Fe(I) on the surface so the formation of a short-lived adduct is likely and in situ spectroelectrochemical measurements of the different complexes studied in the presence of hydrazine might be fruitful. If no adduct were formed, oxidation of hydrazine would occur close to the Fe(II)/(I) formal potential, but as seen in Fig. 2, the foot of the wave is not always close to the formal potential of the catalyst. The reaction in this case should occur at the potential of the oxidation of the adduct (step 3), which is not necessarily close to the Fe(II)/(I) formal potential.

The existence of a maximum in the log I versus $E^{o'}$ plot could also reflect an optimum interaction of the

frontier orbitals of the iron phthalocyanine with the frontier orbitals of hydrazine when the adduct is formed. This could lead to a more favorable electron transfer process from hydrazine to the Fe center since the Fe(II)/(I) formal potential is a reflection of the energy of the frontier orbital bearing a *d*-character, the more positive its value, the more stable the frontier orbital as demonstrated for cobalt phthalocyanines [17, 36].

We provide here possible explanations for the volcano correlations but we are currently investigating alternatives, in order to interpret the significance of the maximum catalytic activities observed, since this is important in predicting activities in terms of simple measurable parameters such as the formal potential of the catalyst.

References

1. Plieth WJ (1978). In Bard AJ (ed) Encyclopedia of electrochemistry of elements, vol VIII. Marcel Dekker, Basel, p 420
2. Bailar JC, Emeleus HJ, Nyholm RS, Trotman-Dickenson AF (eds) (1973) Comprehensive inorganic chemistry. Pergamon, Oxford
3. Golabi SM, Zare HR (1999) J Electroanal Chem 465:168
4. Zagal JH, (1992) Coord Chem Rev 119:89 and references therein
5. Lever ABP (1999) J Porph Phthal 3:488
6. Randin JP (1974) Electrochim Acta 19:83
7. Beck F (1977) J Appl Electrochem 7:191
8. van Veen JAR, Visser, C. (1979) Electrochim Acta 24:921
9. van Veen JAR, van Baar JF, Kroese CJ, Coolegem JGF, de Wit N, Colijn HA (1981) Ber Bunsenges Phys Chem 85:693
10. Zagal JH, Páez M, Tanaka AA, dos Santos JR, Linkous C (1992) J Electroanal Chem 339:13
11. Zagal JH, Gulppi M, Isaacs M, Cárdenas-Jirón G, Aguirre MJ (1998) Electrochim Acta 44:1349
12. Zagal JH, Gulppi M, Caro CA,Cárdenas-Jirón GI (1999) Electrochem. Commun 1:389
13. Cárdenas-Jirón GI, Gulppi MA, Caro CA, Del Rio R, Páez M, Zagal JH, (2001) Electrochim Acta 46:3227
14. Aguirre MJ, Isaacs M, Armijo F, Basáez L, Zagal JH (2002) Electroanalysis 14:356
15. Zagal JH, Gulppi M, Cárdenas-Jirón G (2000) Polyhedron 19:2255
16. Zagal JH, Cárdenas-Jirón G (2000) J Electroanal Chem 489:96
17. Cárdenas-Jirón G, Zagal JH (2001) J Electroanal. Chem 497:55
18. Griveau S, Gulppi M, Bedioui F Zagal JH (2003) Solid State Ionics, in press
19. Ulstrup J (1977) J Electroanal Chem 79:191.
20. Appleby AJ, Savy M, Caro I (1980) J Electroanal Chem 115:267
21. Geraldo D, Linares C, Chen Y-Y, Ureta-Zañartu S, Zagal JH (2002) Electrochem Commun 4:182
22. Weber JH, Bush DM (1965) Inorg Chem 4:469
23. Vilazi S, Nyokong T (2001) J Electroanal Chem 512:56
24. Lever ABP (1993) Inorg Chim Acta 203:171
25. Nevin WA, Liu W, Melnik M, Lever ABP (1986) J Electroanal Chem 213:217
26. Golovin MN, Seymour P.Jayaraj K, Fu YS, Lever ABP (1990) Inorg Chem 29:1719
27. Alexiou C, Lever ABP (2001) Coord Chem Rev 216/217:45 and references therein
28. Tse Y, Janda, P. Lam H, Zhang, J. Pietro W, Lever ABP (1999) J Porph Phthal 1:3
29. Hansch C, Leo A, Taft RW (1991) Chem Rev 91:165
30. Zagal J, Lira S, Ureta-Zañartu S (1986) J Electroanal Chem 210:95
31. Zagal J, Ureta-Zañartu S (1982) J Electrochem Soc 129:2249
32. Zagal J, Muñoz E, Ureta-Zañartu S (1982) Electrochim Acta 27:1373
33. Schreck JO (1971) J Chem Educ 48:103
34. Fierro C, Anderson AB, Scherson DA (1988) J Phys Chem 92:6902
35. Cookson DJ, Smith TD, Boas JF, Hicks PR, Pilbrow JR (1977) J Chem Soc Dalton Trans 109
36. Schlettwein D, Yoshida T (1998) J Electroanal Chem 441:139